Hindawi Publishing Corporation
Journal of Waste Management
Volume 2013, Article ID 632163, 8 pages
http://dx.doi.org/10.1155/2013/632163

Research Article

Adsorption of Cu (II) on the Surface of Nonconventional Biomass: A Study on Forced Convective Mass Transfer in Packed Bed Column

Vishal Mishra,[1,2] Chandrajit Balomajumder,[1] and Vijay Kumar Agarwal[1]

[1] *Department of Chemical Engineering, Indian Institute of Technology, Roorkee 247667, India*
[2] *Department of Chemical Engineering, University of Petroleum and Energy Studies, Dehradun 248007, India*

Correspondence should be addressed to Vishal Mishra; vishal.biochemical@gmail.com

Received 2 January 2013; Accepted 10 February 2013

Academic Editor: Chihpin Huang

Copyright © 2013 Vishal Mishra et al. This is an open access article distributed under the Creative Commons Attribution License, which permits unrestricted use, distribution, and reproduction in any medium, provided the original work is properly cited.

The present investigation has dealt with the adsorption of Cu (II) across liquid phase on the nonconventional adsorbent. The nonconventional adsorbent used in the present work was *Cedrus deodara* sawdust obtained from local carpenter's shop. The maximum uptake capacities of Copper (II) ions at saturation and breakthrough point were 55.63 mg/g and 53.18 mg/g for an initial concentration of 93 mg/L of copper, respectively. The fitting of the experimental data in Langmuir, Freundlich, and Temkin isotherm models indicated the suitability of Langmuir isotherm in terms of very low statistical error functions that is, χ^2 and sum of square errors (SSE) and higher values of (R^2) linear regression coefficient. The goodness of fit of the breakthrough curve in Bohardt-Adams, Wolborska, Modified dose response, and Thomas model indicated the suitability of Thomas model with higher linear regression coefficient and lower values of statistical error functions. The flow rate and bed height affected the hydrodynamic parameters of the packed bed reactor significantly.

1. Introduction

Contamination of water bodies due to heavy metals has posed serious threat to natural flora and fauna. Copper is one of the main constituents of heavy metal series. The Comprehensive Environmental Response, Compensation, and Liability Act (CERCLA) 2011 has ranked Copper at *125*th *position* with a total cumulative score of 805 points [1]. The excessive intake of copper results in bioaccumulation of Cu (II) in digestive organs of humans, *kidney,* mucosal irritation, and anemia [2, 3]. The World Health Organization (WHO) has demarcated the limit of copper (II) in drinking water as 2 mg/L [4]. The wastewater generated from most of the industries like metallurgical units, paints and pigments, alloy and manufacturing, acid mine drainage, and so forth contains huge amount of copper [5, 6]. The excessive concentration of *copper affects* the health of living beings adversely. In past, many conventional technologies like chemical hydroxide precipitation, coagulation and flocculation, cementation, osmosis, reverse osmosis, and so forth have been *practiced* to remove heavy metals from liquid phase [7, 8]. Most of these technologies have been found as very costly and do not work below a minimum concentration of 100 mg/L. Moreover, the usage of these technologies has led to the generation of secondary chemical sludge, *thereby making its disposal undesirable.* However, the removal of heavy metal ions by adsorption process has been studied in detail. Earlier, various sorts of nonconventional adsorbents like litchen, activated carbon, eucalypts leaf powder, and dead bacterium cells have been used for the removal of metal ions [9–11]. Unquestionably, the adsorption mediated by nonconventional adsorbents has contributed significantly in *industrial pollution remediation.* However, most of the studies have concentrated on batch studies and a little importance has been given to continuous column studies. Therefore, the present investigation aimed at sorption of copper ions by nonconventional adsorbent *Cedrus deodara* sawdust in continuous packed bed column studies. Besides, the investigation has also dealt with the

Table 1: Composition of synthetic metal ion solution.

Metal ion	Concentration (mg/L)	Reference
Copper (as Cu (II) ion)	93	[12]

role of hydrodynamic behavior consisting of flow rate and bed height in forced convective mass transfer process, which occurred during upflow of metal ion solution.

2. Materials and Methods

Salts of analytical grade (AR grade) (*Merck Millipore, India* make) of Copper ($CuCl_2$, Copper chloride) were used for preparing synthetic metal ion solution. The initial concentration of copper has been shown in Table 1.

The flow rates of the metal ion solution during the upflow in the packed bed column were kept at 109 mL/h, 160 mL/h, 296 mL/h, and 318 mL/h. The effluent was pumped in the column by peristaltic pump *(Miclins India Limited make)*. The detailed design of the column and instrumentation has been shown in one of our earlier publication [13]. Physicochemical characterization has been provided in one of our publications [14].

2.1. Analysis of Metal Ion and Mathematical Approach. The samples were withdrawn at 15.25, 30.50, 45.75, 60.25, and 75.5 cm at the top of the column. The breakthrough point in breakthrough curve was extrapolated as function of time and the ratio of C_t to C_e, where C_t and C_e are concentrations of copper and zinc ion at time t and at equilibrium in (mg/L).

2.1.1. Mathematical Approach. Equation (1) represents the calculation of uptake capacity, sum of square errors (SSE, statistical error function), and χ^2 (statistical error functions):

$$q = (C_0 - C_e) \times \frac{v}{M},$$
$$\chi^2 = \left(\frac{q_{\text{th}} - q_e}{q_{\text{th}}}\right)^2, \quad (1)$$
$$\text{SSE} = (q_{\text{th}} - q_e)^2,$$

where q_e, q_{th}, and v are experimental and theoretical uptake capacity (mg/g), the volume of feed.

All experiments were carried out in triplicate and average values of data were used.

The breakthrough uptake capacity at break point (T_v) and total capacity of bed (T_c) have been shown in

$$T_v = \int_0^{T_{bp}} \left(1 - \frac{C}{C_0}\right) dt,$$
$$T_c = \int_0^{\infty} \left(1 - \frac{C}{C_0}\right) dt, \quad (2)$$

where C, C_0, and dt were concentration of zinc ions at differential time (dt) and initial concentration of zinc ions.

Table 2: Various isotherm models used in the present investigation.

Name of model	Nonlinear form	Linear form
Langmuir	$q_e = \frac{q_{\max} K_l C_e}{1 + K_l C_e}$	$\frac{C_e}{q_e} = \frac{1}{q_{\max} K_l} + \frac{C_e}{q_{\max}}$
Freundlich	$q_e = (K_f C_e)^{1/n}$	$\text{Log} q_e = \text{Log} K_f + \frac{1}{n} \text{Log} C_e$
Temkin	$q_e = B_t \ln(K_t C_e)$	$q_e = B_t \ln K_t + B_t \ln C_e$

Forced convective mass transfer in the present work has been studied in terms of mass transfer zone (MTZ) was calculated. Equation (3) represents the MTZ in terms of length

$$\text{MTZ} = \left(1 - \frac{T_v}{T_c}\right) h. \quad (3)$$

Adsorption uptake capacities of bed at break point (mg/g) and at saturation (mg/g) were given by (4) and (5) respectively:

$$q_{tb} = \left(\frac{C_0 F T_v}{M}\right), \quad (4)$$

$$q_s = \left(\frac{C_0 F T_c}{M}\right), \quad (5)$$

where C_0, F, and M were initial concentration of zinc ion (mg/L), flow rate (mL/h), and mass of bed (g).

2.1.2. Isotherm and Breakthrough Curve Modeling. Various isotherms such as Langmuir, Freundlich, and Temkin models were used to analyze the goodness of fit of the curve. The equations of Langmuir, Freundlich, and Temkin models have been shown in Table 2 [15, 16].

The modeling of the breakthrough curve was done through Bohardt-Adams, Thomas model, modified dose response model, and Wolborska Model. Table 3 represents the equation of all the abovementioned breakthrough models [17].

The results of the models have been shown in Table 4. The breakthrough curve of metal ion solutions at various flow rates has been shown in Figure 4.

2.1.3. Influence of Flow Rate and Height of Column on Adsorption of Metal Ions. The effect of flow rate was studied on C_t/C_0, mass transfer zone, and various uptake capacities (mg/g). The various flow rates used in the present work were 109 mL/h, 160 mL/h, 296 mL/h, and 318 mL/h, respectively.

2.1.4. Hydrodynamic Behavior Study. In the present investigation, the hydrodynamic behavior of metal ion solution in packed bed column coupled with forced convective mass transfer has been studied with respect to dimensionless numbers such as Sherwood number (Sh), Reynolds number (Re), and Schmidt number (Sc). The empirical correlations

Table 3: Various breakthrough equations used in present investigation.

Model	Equation	Symbols representation
Bohart-Admas	$\frac{C_t}{C_i} = \exp\left[k_{ba}C_i t - k_{ba}N_0\frac{Z}{W}\right]$	Where C_t, C_i, k_{ba}, N_0, Z, and W were concentration of zinc at time t, initial concentration of zinc, kinetic constant (L/mg·min), saturation concentration (g/L), bed height of column (cm), flow rate of the fluid (mL/h)
Wolborska model	$\frac{C_t}{C_i} = \exp\left[\frac{\beta_a C_i t}{N_0} - \frac{\beta_a Z}{W}\right]$	Where β_a is kinetic coefficient of external mass transfer (L/h), and the rest of all the parameters are the same as shown in Bohart-Admas model
Modified dose response model	$\frac{C_t}{C_i} = 1 - \frac{1}{1 + [V_{eff}/b_{mdr}]^{a_{mdr}}}$	Where V_{eff} is the volume (L) of metal ion solution, and a_{mdr} and b_{mdr} are model constants
Thomas model	$\frac{C_t}{C_i} = \frac{1}{1 + \exp\left[k_{Th}q_0(M/F) - k_{Th}t\right]}$	Where q_0, k_{Th}, C_t, C_i, M, and F are metal uptake capacity (mg/g), model constant (L/mg·h), metal ion concentration at time t (mg/L), influent metal ion concentration (mg/L), mass of the biomass packed in the column (g), and F (mL/h) is the flow rate of metal solution through packed bed

Table 4: Study of Langmuir, Freundlich, and Temkin isotherm.

Name of model	Concentration of Cu (II) ion (mg/L)	Model equation	Linear regression coefficient (R^2)
Langmuir isotherm	93	$y = -17.566x + 115.69$	$R^2 = 0.8657$
Freundlich isotherm	93	$y = 1.0714x + 0.3295$	$R^2 = 0.8171$
Temkin isotherm	93	$y = 0.0237x + 1.0117$	$R^2 = 0.5108$

for the abovementioned dimensionless number have been shown in (6) and (7), respectively [18]:

$$\mathrm{Sh} = J_D R_e \mathrm{Sc}^{1/3}, \quad (6)$$

$$\frac{\mathrm{Sh}}{\mathrm{Sc}} = \left[\frac{k.\rho.y}{Q}\right] R_e, \quad (7)$$

where J_D, k, ρ, and y are Clinton-Colbourn factor, mass transfer coefficient (m/s), density of solution, and mass fraction of the component, respectively.

3. Results and Discussion

The results of isotherm modeling have been shown in Figures 1, 2, and 3 and Tables 4 and 5.

It became evident from Tables 4 and 5 and Figures 1, 2, and 3 that among all the isotherm models for Cu (II) ions, both Langmuir and Freundlich isotherms have better *efficiency* to describe the sorption of Cu (II) ion on the surface of CDS. In between both the isotherms, Langmuir isotherm was found comparatively more suitable to interpret the binding of metal (Cu (II)) ion on the surface of CDS. The outcome of Temkin model application (Tables 4 and 5, and Figure 3) did not yield the suitable explanation of sorption of Cu (II) ion on the surface of the CDS. The results showed that the applicability of Temkin isotherm model ruled in very high values of statistical error functions coupled with significantly

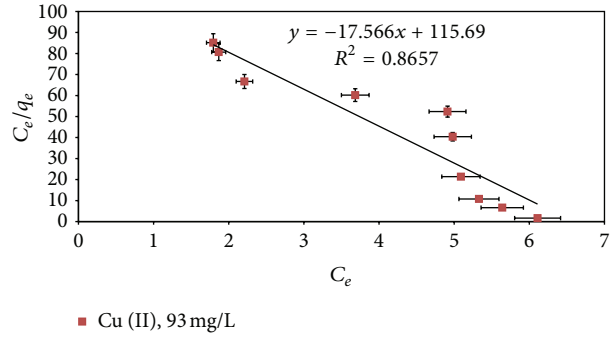


Figure 1: Study of Langmuir isotherm model.

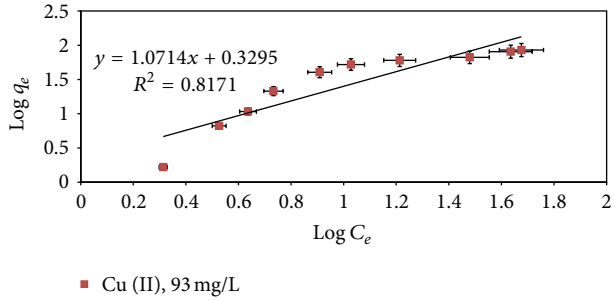


Figure 2: Study of Freundlich isotherm model.

Table 5: Study of Langmuir, Freundlich, and Temkin isotherm (calculation of model constants and error functions).

Name of the model				
Langmuir isotherm	Q_{max} (mg/g)	K_l (l mg^{-1})	Sum of square errors (SSE)	χ^2
For Cu	0.056	0.154	36.33	13.34
Freundlich isotherm	K_f	$1/n$	Sum of square errors (SSE)	χ^2
For Cu	2.13	0.933	48.14	18.9
Temkin isotherm	B_t	K_t	Sum of square errors (SSE)	χ^2
For Cu	0.0273	10.27	77.84	40.36

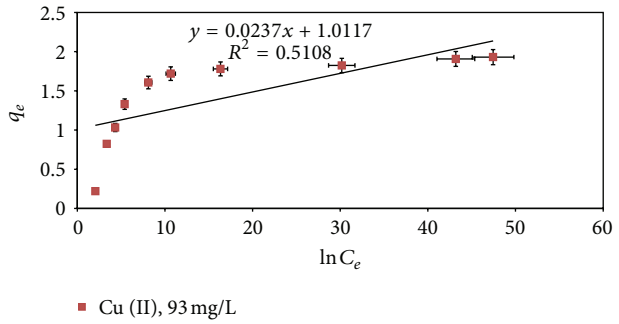


Figure 3: Study of Temkin isotherm model.

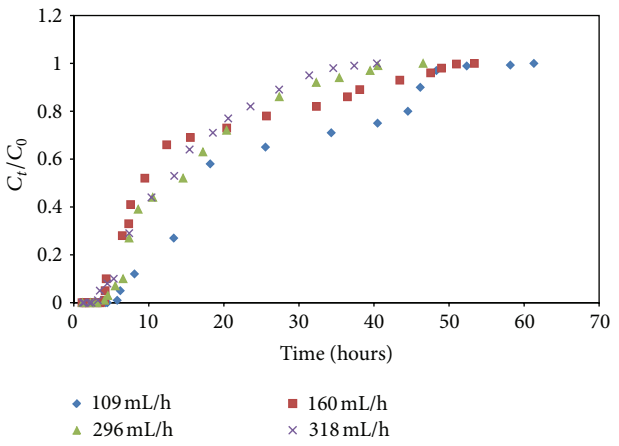


Figure 4: Study of breakthrough curve at various flow rates.

lower value of goodness of fit of the curve or linear regression coefficient.

3.1. Effect of Flow Rate and Height of Packed Bed on Sorption of Cu (II) Ion. In the present investigation, four different flow rates, that is, 109 mL/h, 160 mL/h, 296 mL/h, and 318 mL/h were used to plot the breakthrough between C_t/C_0 and time (measured in hours). The concentration of Cu (II) ion 93 (mg/L) was used throughout the continuous column study. The column was kept in double-walled isotherm chamber. The temperature of the chamber was set at 30°C ± 0.5°C. The breakthrough curve has been shown in Figure 4.

It became evident from Figure 4 that the increase in flow rate significantly reduced the time to achieve the breakthrough point in breakthrough curve. The reduction in time to achieve the breakthrough point relatively at higher flow rates was due to the less time of contact between particles of the bed and the metal ion solution. Mishra et al. [13] and Ostroski et al. [19] have reported the similar kind of results showing the effect of flow rate on adsorption of Zn (II) and Fe (III) on the surface of immobilized bacterium and Zeolite NaY, respectively.

3.2. Influence of Height of Column (in cm) and Flow Rate (in mL/h) on Adsorption of Cu (II) Ion. Table 6 represents the effect of flow rate and height of the column on mass transfer zone (MTZ), saturation uptake capacity, and break point uptake capacity (mg/g).

It became evident from Table 6 that there was an increase in mass transfer zone (MTZ, cm) of the packed bed with the increase in flow rate from 109 mL/h to 318 mL/h and height of the column. The maximum removal of Cu (II) ion was obtained at 109 mL/h. Moreover, there was substantial decrease in the saturation uptake capacities and break point uptake capacities of the bed with simultaneous increase in flow rate and height of bed. The decrease in both the uptake capacities was due to the fact that the increase in flow rate led to the reduced contact time between the metal ion solution and adsorbent bed. Moreover, the decrease in both the uptake capacities with the increase of bed height was due to the change in volume to mass ratio of adsorbent.

It became evident from the outcome of Tables 7 and 8 that, except Thomas model, none of the other models led to the satisfactory explanation of breakthrough curve. The value of linear regression coefficient (R^2) for Thomas model was relatively high against Bohart-Adams model, Wolborska model, and modified dose response model. With the increase of bed height there was simultaneous increase in Thomas model constant, k_{th}. However, with an increase in flow rate, there was a decrease in Thomas model constant, k_{th}. The rationale behind the decrease of model constant was reduction in contact time of feed solution with the adsorbent particles at higher flow rates. Moreover, the Thomas model uptake capacity (q_0) (Table 8) was very closer to the saturation uptake capacity q_s, derived experimentally from (5). This further confirmed the suitability of the Thomas model over other breakthrough models used in the present investigation. With the repertoire of these modeling data, there were some interesting features of designed column that appeared, which were as follows (a) the increase in flow rate of Cu (II) ion inside the column led to the decrease in saturation concentration (N_0), (b) the increase in bed height resulted

Table 6: Influence of flow rate (mL/h) and height of column on sorption of Zn (II) ion.

Flow rate (mL/h)	Height of column	Mass transfer zone (MTZ, cm)	q_s (mg/g)	q_{tb} (mg/g)	χ^2 (q_s)	χ^2 (q_{tb})	SSE (q_s)	SSE (q_{tb})
	15.25	3.38	55.63	53.18	0.01	0.07	0.16	0.29
	30.5	11.33	53.11	50.11	0.04	0.05	0.18	0.33
109	45.75	29.33	50.33	48.67	0.09	0.07	0.19	0.14
	60	47.88	46.77	43.77	0.33	0.04	0.91	0.11
	75.5	62.38	42.11	39.19	0.14	0.05	0.41	0.21
	15.25	4.41	52.88	47.33	0.04	0.06	0.33	0.31
	30.5	14.55	48.11	44.56	0.06	0.05	0.15	0.18
160	45.75	32.87	46.17	42.11	0.09	0.09	0.18	0.22
	60	49.77	42.13	40.19	0.11	0.06	0.13	0.17
	75.5	64.33	40.19	37.33	0.19	0.17	0.19	0.11
	15.25	5.58	50.13	46.41	0.02	0.09	0.51	0.77
	30.5	16.71	46.18	42.19	0.07	0.19	0.17	0.11
296	45.75	33.14	44.11	40.33	0.11	0.36	0.18	0.88
	60	53.44	40.19	38.11	0.31	0.44	0.55	0.55
	75.5	67.18	38.11	35.22	0.44	0.91	0.19	0.33
	15.25	6.77	48.13	43.18	0.07	0.77	0.44	0.11
	30.5	19.33	46.13	39.11	0.17	0.34	0.15	0.77
318	45.75	37.44	42.17	35.15	0.08	0.51	0.66	0.19
	60	48.11	38.17	34.11	0.04	0.66	0.17	0.87
	75.5	70.14	33.11	30.18	0.05	0.54	0.18	0.73

Table 7: Modeling of breakthrough curve.

Flow rate (mL/h)	Bed height (cm)	Bohart-Adams model					Wolborska model			
		$k_{ba} \times 10^{-3}$ (L /mg/h)	N_0 (mg/L)	R^2	χ^2	SSE	β_a	R^2	χ^2	SSE
	15.25	37.88	66.73	0.84	3.26	5.51	6.33	0.55	7.45	10.44
	30.5	36.17	73.33	0.77	4.41	6.63	5.53	0.71	7.88	10.77
109	45.75	32.33	78.17	0.65	5.59	8.55	4.11	0.66	8.55	11.91
	60	30.18	82.77	0.54	3.33	7.08	6.19	0.48	6.70	12.34
	75.25	27.33	88.19	0.71	4.28	6.33	7.88	0.59	7.71	10.11
	15.25	35.38	62.88	0.71	4.43	6.18	5.17	0.77	8.18	11.26
	30.5	33.11	64.11	0.82	5.51	8.22	7.33	0.84	7.55	12.32
160	45.75	30.17	67.02	0.76	3.38	7.84	5.44	0.74	6.92	10.33
	60	27.76	69.38	0.73	3.19	8.92	2.34	0.72	7.73	11.38
	75.25	25.33	71.38	0.55	4.17	9.02	6.11	0.70	7.84	11.93
	15.25	34.18	58.33	0.77	6.33	7.51	1.48	0.66	6.64	5.58
	30.5	31.67	61.24	0.88	7.88	8.44	3.33	0.54	5.53	6.77
296	45.75	28.16	63.48	0.90	8.19	9.19	5.18	0.77	7.73	10.11
	60	25.11	65.19	0.81	8.77	10.11	6.17	0.81	6.66	9.33
	75.25	23.41	67.33	0.71	4.71	7.73	7.12	0.33	4.33	6.33
	15.25	31.77	55.18	0.75	5.55	6.11	3.38	0.48	3.38	5.18
	30.5	28.77	57.04	0.33	5.64	7.91	4.43	0.55	4.41	6.44
318	45.75	25.33	60.09	0.44	7.18	9.22	5.51	0.71	5.53	7.33
	60	22.11	62.88	0.57	8.11	10.16	6.67	0.66	6.33	8.12
	75.25	20.17	64.33	0.66	3.19	11.24	3.38	0.67	7.21	7.07

Table 8: Modeling of breakthrough curve.

Flow rate (mL/h)	Bed height (cm)	Thomas model					Modified dose response model				
		k_{th}	q_0	R^2	χ^2	SSE	b_{mdr}	a_{mdr}	R^2	χ^2	SSE
109	15.25	0.37	56.11	0.99	0.01	0.04	1.95	11.18	0.88	1.12	2.24
	30.5	0.43	54.11	0.99	0.03	0.06	1.39	16.33	0.79	1.56	3.29
	45.75	0.56	52.31	0.98	0.01	0.07	0.89	18.11	0.66	1.77	4.88
	60	0.62	49.55	0.97	0.00	0.04	2.11	20.17	0.61	1.81	5.78
	75.25	0.77	47.11	0.99	0.03	0.08	2.44	15.33	0.55	1.97	6.77
160	15.25	0.35	53.11	0.99	0.01	0.04	1.78	16.71	0.57	1.44	3.31
	30.5	0.40	50.18	0.98	0.05	0.02	1.66	19.05	0.91	1.55	3.44
	45.75	0.47	47.17	0.97	0.08	0.07	1.49	23.08	0.57	1.67	4.67
	60	0.57	42.11	0.99	0.03	0.06	1.61	20.05	0.69	1.78	6.17
	75.25	0.63	40.55	0.94	0.00	0.00	1.55	12.38	0.55	1.85	5.66
296	15.25	0.33	51.11	0.99	0.04	0.01	1.71	13.44	0.66	1.77	3.38
	30.5	0.43	47.19	0.97	0.07	0.09	1.62	16.77	0.87	2.22	5.17
	45.75	0.47	45.11	0.96	0.05	0.07	1.31	17.19	0.88	2.19	5.17
	60	0.51	40.19	0.99	0.07	0.06	1.82	19.18	0.79	2.44	6.16
	75.25	0.53	37.33	0.98	0.08	0.09	1.77	11.09	0.76	2.67	4.44
318	15.25	0.29	50.11	0.99	0.05	0.06	1.68	8.11	0.71	3.31	6.67
	30.5	0.37	48.17	0.96	0.09	0.09	1.57	12.38	0.65	4.14	4.55
	45.75	0.42	44.24	0.97	0.07	0.01	1.91	15.06	0.55	6.11	5.68
	60	0.47	40.19	0.96	0.06	0.08	1.33	19.11	0.88	5.56	6.77
	75.25	0.51	37.55	0.93	0.09	0.07	1.88	11.33	0.76	5.13	7.19

Table 9: Hydrodynamic behavior of fluid flow inside packed bed column.

Flow rate (mL/h)	Bed height (cm)	R_e	S_c	S_h	$k \times 10^{-4}$ (m/s)
109	15.25	0.68	27.33	6.67	15.55
	30.5	0.63	23.33	5.97	11.13
	45.75	0.59	17.37	5.77	9.33
	60	0.54	13.33	5.66	7.84
	75.25	0.49	11.76	5.19	6.16
160	15.25	0.73	30.19	7.84	19.39
	30.5	0.68	27.39	6.84	16.77
	45.75	0.62	24.52	5.52	15.25
	60	0.58	22.19	4.33	12.31
	75.25	0.52	20.65	3.17	10.33
296	15.25	0.77	34.83	8.89	24.41
	30.5	0.69	32.19	7.71	23.18
	45.75	0.64	29.23	6.54	20.33
	60	0.62	27.73	5.61	18.24
	75.25	0.57	23.36	4.33	17.19
318	15.25	0.83	38.59	9.19	30.06
	30.5	0.76	35.55	8.52	28.16
	45.75	0.72	32.17	7.31	25.41
	60	0.69	30.19	6.72	21.33
	75.25	0.64	27.17	5.44	18.19

Table 10: Comparative study of sorption of Cu (II) ion.

Name of the adsorbent	Uptake capacity (mg/g)	Reference
Caulerpa lentillifera	10.738	[20]
Asylum discolor (Native)	6.15	[3]
Asylum discolor (Acid treated)	17.18	[3]
Olive stone	1.97	[21]
Pine bark	11.94	[21]
CDS	55.63–30.18	This study

in an increase in bed saturation concentration (N_0), and (c) mass transfer hindrance factor (diffusion resistance, k_{ba}) increased with the flow rate. The diffusion resistance pursued a negative trend with the increase in bed height at all the flow rates.

3.3. Hydrodynamic Behavior of Fluid Flow inside the Packed Bed Column at Various Flow Rates and Bed Heights. The hydrodynamic behavior of fluid flow inside the column has been shown in Table 9.

It became evident from the Table 9 that the dimensionless parameters varied significantly with flow rate of the metal ion solution inside the packed bed and *bed height*. With the increase of flow rate there was a significant rise in the velocity of fluid inside the column, Reynolds number, Schmidt number, and Sherwood number. However, with the increase of bed height at fixed flow rate, there was a decrease in velocity of the metal ion solution inside the bed, Reynolds number, Schmidt number, and Sherwood number. The decrease in the values of these forced convective (inter phase) mass transfer parameters was due to the path resistance posed by the particles of bed, and this resistance increased with the increase of bed height and reduced when the flow rate is high. Therefore, in the present investigation it was summarized that large flow rates and smaller bed heights rendered the minimum possible resistance for the transfer of metal ions from liquid phase to packed bed. Table 10 represents the comparative analysis of uptake capacities of various adsorbents.

It became evident from Table 10 that adsorbent used in present investigation has tremendous potential to adsorb Cu (II) ions from liquid phase.

4. Conclusion

The investigation has been undertaken to evaluate the biosorption potential of *Cedrus deodara sawdust* (CDS) in terms of sorption of Cu (II) ion in packed bed column studies. The maximum uptake capacity at saturation and at break points was 55.63 (mg/g) and 53.18 (mg/g), respectively, obtained at 109 mL/h and 15.25 cm. At various flow rates (109 mL/h–308 mL/h) and bed heights, the Langmuir and Thomas models were found relatively more suitable to explain the sorption of Cu (II) ion in terms of isotherm model and breakthrough curve modeling. However, the flow rate and height of the packed bed significantly affected the saturation concentration (N_0), diffusion resistance (k_{ba}), and hydrodynamic properties of the column reactor. The investigation ends up with the recommendations for various industrial partners to utilize the advantages of the packed bed column reactor designed in present work for the purpose removal of copper ions from industrial effluent.

Acknowledgments

The authors are very grateful to Ministry of Human Resource Development, New Delhi, India, and Institute Instrumentation Center for extending their financial and technical support.

References

[1] Detailed data for 2011 priority list of hazardous substances ATSDR, division of toxicology and environmental medicine.

[2] G. Blazquez, M. A. Martín-Lara, E. Dionisio-Ruiz, G. Tenorio, and M. Calero, "Evaluation and comparison of the biosorption process of copper ions onto olive stone and pine bark," *Journal of Industrial and Engineering Chemistry*, vol. 17, no. 5-6, pp. 824–833, 2011.

[3] G. Bayramoglu, A. G. Yakup, and N. Adiguzel, "Removal of Ni (II) and Cu (II) ions using native and acid treated Ni-hyperaccumulator plant Alyssum discolor from Turkish serpentine soil," *Chemosphere*, vol. 89, no. 3, pp. 302–309, 2012.

[4] T. Şahana, H. Ceylan, N. Şahiner, and N. Aktaşa, "Optimization of removal conditions of copper ions from aqueous solutions by *Trametes versicolor*," *Bioresource Technology*, vol. 101, no. 12, pp. 4520–4526, 2010.

[5] M. A. Hashim, S. Mukhopadhyay, J. N. Sahu, and B. Sengupta, "Remediation technologies for heavy metal contaminated groundwater," *Journal of Environmental Management*, vol. 92, no. 10, pp. 2355–2388, 2011.

[6] G. M. Gadd, "Biosorption: critical review of scientific rationale, environmental importance and significance for pollution treatment," *Journal of Chemical Technology and Biotechnology*, vol. 84, no. 1, pp. 13–28, 2009.

[7] A. Sari and M. Tuzen, "Biosorption of total chromium from aqueous solution by red algae (*Ceramium virgatum*): equilibrium, kinetic and thermodynamic studies," *Journal of Hazardous Materials*, vol. 160, no. 2-3, pp. 349–355, 2008.

[8] A. Sari, D. Mendil, M. Tuzen, and M. Soylak, "Biosorption of Cd(II) and Cr(III) from aqueous solution by moss (*Hylocomium splendens*) biomass: equilibrium, kinetic and thermodynamic studies," *Chemical Engineering Journal*, vol. 144, no. 1, pp. 1–9, 2008.

[9] O. D. Uluozlu, A. Sari, M. Tuzen, and M. Soylak, "Biosorption of Pb(II) and Cr(III) from aqueous solution by lichen (*Parmelina tiliaceae*) biomass," *Bioresource Technology*, vol. 99, no. 8, pp. 2972–2980, 2008.

[10] V. Mishra, C. Balomajumder, and V. K. Agarwal, "Sorption of Zn (II) ion onto the surface of activated carbon derived from eucalyptus bark saw dust from industrial wastewater: isotherm, kinetics, mechanistic modeling, and thermodynamics," *Desalination and Water Treatment*, vol. 46, no. 1–3, pp. 332–352, 2012.

[11] V. Mishra, C. Balomajumder, and V. K. Agarwal, "Zn(II) ion biosorption onto surface of eucalyptus leaf biomass: isotherm, Kinetic, and mechanistic modeling," *Clean—Soil, Air, Water*, vol. 38, no. 11, pp. 1062–1073, 2010.

[12] C. A. Basha, S. J. Selvi, E. Ramasamy, and S. Chellammal, "Removal of arsenic and sulphate from the copper smelting industrial effluent," *Chemical Engineering Journal*, vol. 141, no. 1–3, pp. 89–98, 2008.

[13] V. Mishra, C. Balomajumder, and V. K. Agarwal, "Simultaneous adsorption and bioaccumulation: a study on continuous mass transfer in column reactor," *Environmental Progress and Sustainable Energy*, 2012.

[14] V. Mishra, C. Balomajumder, and V. K. Agarwal, "Kinetics, mechanistic and thermodynamics of Zn (II) Ion sorption: a modeling approach," *Clean Soil Air and Water*, vol. 40, no. 7, pp. 718–727, 2012.

[15] R. A. Anayurt, A. Sari, and M. Tuzen, "Equilibrium, thermodynamic and kinetic studies on biosorption of Pb(II) and Cd(II) from aqueous solution by macrofungus (*Lactarius scrobiculatus*) biomass," *Chemical Engineering Journal*, vol. 151, no. 1–3, pp. 255–261, 2009.

[16] A. Sari and M. Tuzen, "Kinetic and equilibrium studies of biosorption of Pb(II) and Cd(II) from aqueous solution by macrofungus (*Amanita rubescens*) biomass," *Journal of Hazardous Materials*, vol. 164, no. 2-3, pp. 1004–1011, 2009.

[17] A. Singh, D. Kumar, and J. P. Gaur, "Continuous metal removal from solution and industrial effluents using *Spirogyra* biomass-packed column reactor," *Water Research*, vol. 46, no. 3, pp. 779–7788, 2012.

[18] H. Kasaini and R. K. Mbaya, "Continuous adsorption of Pt ions in a batch reactor and packed-bed column," *Hydrometallurgy*, vol. 97, no. 1-2, pp. 111–118, 2009.

[19] I. C. Ostroski, M. A. S. D. Barros, E. A. Silva, J. H. Dantas, P. A. Arroyo, and O. C. M. Lima, "A comparative study for the ion exchange of Fe(III) and Zn(II) on zeolite NaY," *Journal of Hazardous Materials*, vol. 161, no. 2-3, pp. 1404–1412, 2009.

[20] R. Apiratikul, V. Madacha, and P. Pavasant, "Kinetic and mass transfer analyses of metal biosorption by *Caulerpa lentillifera*," *Desalination*, vol. 278, no. 1–3, pp. 303–311, 2011.

[21] G. Blázquez, M. A. Martín-Lara, E. Dionisio-Ruiz, G. Tenorio, and M. Calero, "Evaluation and comparison of the biosorption process of copper ions onto olive stone and pine bark," *Journal of Industrial and Engineering Chemistry*, vol. 17, no. 5-6, pp. 824–833, 2012.